ELSEVIER

International Journal of Solids and Structures 41 (2004) 3255–3274

INTERNATIONAL JOURNAL OF SOLIDS and STRUCTURES

www.elsevier.com/locate/ijsolstr

A piezoelectric screw dislocation interacting with an interphase layer between a circular inclusion and the matrix

Y.W. Liu [a,*], Q.H. Fang [a], C.P. Jiang [b]

[a] *Department of Engineering Mechanics, Hunan University, Yuelu, Changsha 410082, PR China*
[b] *Beijing University of Aeronautics and Astronautics, Beijing 100083, PR China*

Received 7 April 2003; received in revised form 17 November 2003

Available online 26 February 2004

Abstract

The interaction of a piezoelectric screw dislocation with an interphase layer between the circular inclusion and the piezoelectric matrix is dealt with. An efficient method for multiplying connected region is developed by combining the sectional holomorphic function, Cauchy-type integral and Laurent series expansion techniques, in terms of which the relation among the complex potentials for the three material regions is obtained. The functional equation in complex potentials for the interphase layer is derived, resulting in explicit series solutions for the two cases when piezoelectric screw dislocation is located in the matrix or in the inclusion. The image force acting on the piezoelectric screw dislocation is calculated by using the generalized Peach–Koehler formula. Three practical cases are provided to investigate the influence of the interphase layer parameters on the image force. The present solutions contain a number of novel and previously known results which can be shown to be special cases.

Keywords: Piezoelectric screw dislocation; Inhomogeneous materials; Interphase layer; Complex potential method

1. Introduction

The solution of the appropriate problem involving the interaction of dislocations with inclusions plays a fundamental role in many practical and theoretical applications, namely, it increases the understanding of material defects thereby providing valuable insight into the mechanical behavior of materials (Sudak, 2003a). All materials of engineering importance, from quenched and tempered steels to fiber or laminated reinforced composites, are heterogeneous systems. The second phase inclusions or dispersed particles provide barriers to the dislocation motion and thus affect the flow stress and strain hardening behavior of the materials. With the daily emerging of new material systems, theoretical analysis becomes increasingly valuable. In addition, it can be used to study the crack growth in composites, as well as strengthening and

* Corresponding author. Tel.: +86-7318821889; fax: +86-7318822330.
E-mail address: liuyouw8294@sina.com (Y.W. Liu).

0020-7683/$ - see front matter © 2004 Elsevier Ltd. All rights reserved.
doi:10.1016/j.ijsolstr.2003.12.027

hardening mechanisms in alloyed materials. In view of its importance, a number of contributions have been conducted on this problem during the last several decades, and the references listed herein (Dundurs and Mura, 1964; Dundurs and Sendeckyj, 1965; Barnett and Tetelman, 1966; Smith, 1968; Sendeckj, 1970; Luo and Chen, 1991; Gong and Meguid, 1994; Zhang and Qian, 1996; Xiao and Chen, 2000, 2001, 2002; Wang and Shen, 2002; Sudak, 2003a; Liu et al., 2003; Jiang et al., 2003; Fang et al., 2003) are just some examples of contributions in this area.

In recent years, piezoelectric materials have become an important branch of modern engineering materials due to the fact that they have potentials for use in many modern devices and composite structures. Their favorable electromechanical coupling effect presents a level of difficulty not found in designs and analyses of mechanical behaviors of composite materials. The electroelastic interaction of dislocations and inclusions plays a significant role in studying the electromechanical coupling behavior of piezoelectric materials, and it is motivated rapidly in the fields of solid mechanics and materials science. As a result, a considerable amount of attention has been paid to this problem. Kattis et al. (1998) investigated the electro–elastic interaction effects of a piezoelectric screw dislocation with circular inclusion in piezoelectric material. Meguid and Deng (1998) and Deng and Meguid (1999) considered the problem involving the interaction between the piezoelectric elliptical inhomogeneity and a screw dislocation, which is located inside or outside inhomogeneity under antiplane shear and in-plane electric field. The interaction between a piezoelectric screw dislocation and elliptical inclusion is studied by Liu et al. (2000). Huang and Kuang (2001) evaluated the generalized electromechanical force when the dislocation locates inside, outside or on the interface of the elliptical inhomogeneity in a infinite piezoelectric media. The electroelastic interaction between a piezoelectric screw dislocation, which is located either outside or inside inhomogeneity and circular interfacial rigid lines under antiplane mechanical and in-plane electrical loads in linear piezoelectric materials, is dealt with by Liu and Fang (2003).

In the above studies involving the electroelastic interaction of the dislocation with the inclusion in piezoelectric solids, most analytical solutions are restricted to two-phase model, namely, the interfaces are assumed as idealized ones with zero thickness. Due to the presence of materials such as fiber coating or transitional layers between the inclusion and the matrix, it is more reasonable to regard an interface as interphase layer with finite thickness. The importance of three-phase model (inclusion-interphase-matrix model) in piezoelectric materials has been described by Sudak (2003b). Referring to the work by Liu et al. (2003), this paper will focus on the electroelastic interaction of a piezoelectric screw dislocation with an interphase layer between the circular inclusion and the infinite matrix.

The complex potentials (Muskhelishvili, 1975) are used to deal with the problem. For a three-phase model (such as inclusion-interphase-matrix model), under remote homogeneous stress and electric fields, closed form solutions can often be obtained (see, for example, Wang and Shen, 2001; Jiang et al., 2001; Sudak, 2003b). However, for problems with singularities, mathematical difficulties are encountered. In this paper an effective method for multiplying connected region is developed by combining the sectional holomorphic function, Cauchy-type integral and Laurent series expansion techniques. The relation among the complex potentials for the three material regions is given and the functional equation in complex potential for interphase layer is derived, resulting in explicit series solutions for the two cases when the piezoelectric screw dislocation is located in the matrix or in the inclusion. The image force acting on the piezoelectric screw dislocation is calculated by using the generalized Peach–Koehler formula. Finally, the influence of the interphase layer parameters (electroelasticity modulus, thickness) on the dislocation force is examined for three practical cases. Results presented in this paper contain the previous known solutions as special cases. The obtained explicit solutions can be used as Green's functions to solve the problem of electroelastic interaction between the coated inclusion and the arbitrary shape crack inside the matrix or the inclusion.

2. Problem statement and basic formulation

Let us consider an infinite piezoelectric medium containing a circular inclusion and an annular interphase layer, as shown in Fig. 1, where R_1 and R_2 are the inner and outer radii of the interphase annulus. The matrix, inclusion and interphase layer are assumed to be transversely isotropic piezoelectric media which have been poled along the z-direction with an isotropic xoy-plane. A piezoelectric screw dislocation $\mathbf{b} = \{b_z, b_\varphi\}^{\mathrm{T}}$ (Pak, 1990; Liu et al., 2000) is located at arbitrary point z_0, which is located either in the matrix or in the inclusion (z_0 is plotted in the matrix in Fig. 1). Where an interface exists between two dissimilar materials, we assume perfect bonding. Additionally, we assume no mechanical and electric loads at infinity.

For the present problem, out-of-plane displacement and in-plane electric field need to be considered, so that there are only non-trivial displacement w, strains γ_{xz} and γ_{yz}, stresses τ_{xz} and τ_{yz}, electric potential φ, electrical field components E_x and E_y and electric displacement components D_x and D_y in the local Cartesian coordinates. All components are only functions of x and y. The mechanical and electric coupled constitutive relations (Tiersten, 1969) can be expressed as:

$$\tau_{xz} = C_{44}\frac{\partial w}{\partial x} + e_{15}\frac{\partial \varphi}{\partial x} \quad \tau_{yz} = C_{44}\frac{\partial w}{\partial y} + e_{15}\frac{\partial \varphi}{\partial y} \tag{1}$$

$$D_x = e_{15}\frac{\partial w}{\partial x} - d_{11}\frac{\partial \varphi}{\partial x} \quad D_y = e_{15}\frac{\partial w}{\partial y} - d_{11}\frac{\partial \varphi}{\partial y} \tag{2}$$

where C_{44} is the longitudinal shear modulus at a constant electric field, e_{15} is the piezoelectric modulus, d_{11} is the dielectric modulus at a constant stress field.

The equilibrium equation and charge equation can be reduced to the harmonic equations

$$\nabla^2 w = 0 \quad \nabla^2 \varphi = 0 \tag{3}$$

where $\nabla^2 = \partial^2/\partial x^2 + \partial^2/\partial y^2$ is the two-dimensional Laplace operator.

Referring to the work by Jiang et al. (2001), we introduce the vector of generalized displacement $\mathbf{U} = \begin{Bmatrix} w \\ \varphi \end{Bmatrix}$. Substituting it into Eq. (3), we obtain

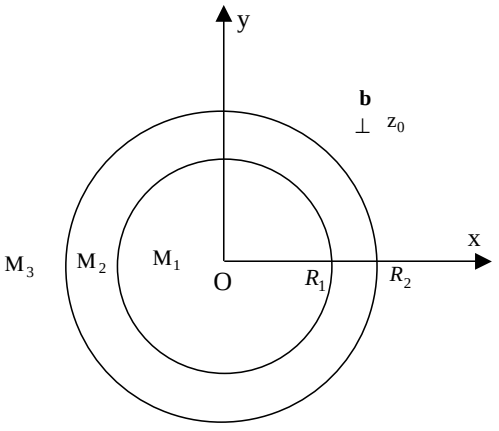

Fig. 1. A piezoelectric screw dislocation interacting with the inclusion and interphase layer.

$$\nabla^2 \mathbf{U} = 0 \tag{4}$$

Introducing the following vectors of generalized stress and strain:

$$\mathbf{\Sigma}_x = \begin{Bmatrix} \tau_{xz} \\ D_x \end{Bmatrix} \quad \mathbf{\Sigma}_y = \begin{Bmatrix} \tau_{yz} \\ D_y \end{Bmatrix} \tag{5}$$

$$\mathbf{Y}_x = \begin{Bmatrix} \gamma_{xz} \\ -E_x \end{Bmatrix} \quad \mathbf{Y}_y = \begin{Bmatrix} \gamma_{yz} \\ -E_y \end{Bmatrix} \tag{6}$$

By adopting the above notations and noting $E_i = -\varphi_{,i}$, Eqs. (1) and (2) can be unified into

$$\mathbf{\Sigma}_x = M\mathbf{Y}_x \quad \mathbf{\Sigma}_y = M\mathbf{Y}_y \tag{7}$$

where $M = \begin{bmatrix} C_{44} & e_{15} \\ e_{15} & -d_{11} \end{bmatrix}$.

Eq. (4) shows that the general solution of the generalized displacement vector $\mathbf{U}$ can be expressed by a generalized analytical function vector $\mathbf{f}(z)$, where $z = x + \mathrm{i}y$ is the complex variable.

$$\mathbf{U} = \mathrm{Re}\,\mathbf{f}(z) \tag{8}$$

where Re denotes the real part of the complex function, and

$$\mathbf{f}(z) = \begin{Bmatrix} f_w(z) \\ f_\varphi(z) \end{Bmatrix} \tag{9}$$

$f_w(z)$ and $f_\varphi(z)$ are conventional analytical functions.

Considering Eq. (8), the constitutive relations Eq. (7) can be expressed as

$$\mathbf{\Sigma}_x - \mathrm{i}\mathbf{\Sigma}_y = M\mathbf{F}(z) \tag{10}$$

where $\mathbf{F}(z) = \mathbf{f}'(z)$ and the superscript prime denotes derivative with respect to argument z.

Hence, the mechanical stresses and the electric displacements can be expressed in terms of $f_w(z)$ and $f_\varphi(z)$ as follows:

$$\tau_{xz} - \mathrm{i}\tau_{yz} = C_{44} f'_w(z) + e_{15} f'_\varphi(z) \tag{11}$$

$$D_x - D_y = e_{15} f'_w(z) - d_{11} f'_\varphi(z) \tag{12}$$

In order to facilitate the analysis, we introduce the following function vector:

$$\mathbf{T} = \int_{\mathrm{A}}^{\mathrm{B}} (\mathbf{\Sigma}_x \,\mathrm{d}y - \mathbf{\Sigma}_y \,\mathrm{d}x) = M\mathrm{Im}[\mathbf{f}(z)]_{\mathrm{A}}^{\mathrm{B}} \tag{13}$$

where $[\cdot]_{\mathrm{A}}^{\mathrm{B}}$ is the change in the bracketed function vector in from point A to point B along any arc AB (not pass through interfaces of dissimilar phase).

The assumption of perfect bonging between two adjacent materials implies the continuity of generalized displacement and stress vectors across the interface, which leads to the following continuity conditions:

$$\mathbf{T}_1 = \mathbf{T}_2 \quad \mathbf{U}_1 = \mathbf{U}_2 \quad \text{on } |t| = R_1 \tag{14}$$

$$\mathbf{T}_2 = \mathbf{T}_3 \quad \mathbf{U}_2 = \mathbf{U}_3 \quad \text{on } |t| = R_2 \tag{15}$$

where and hereafter the subscripts 1, 2 and 3 refer to the inclusion, the interphase layer and the matrix, respectively.

For the convenience of analysis, the following new analytical function vectors are introduced in the corresponding region according to the Schwarz symmetry principle.

$$\mathbf{f}_{1*}(z) = -\overline{\mathbf{f}_1}(R_1^2/z) \quad \text{for} \quad |z| > R_1 \tag{16}$$

$$\mathbf{f}_{2*}(z) = -\overline{\mathbf{f}_2}(R_1^2/z) \quad \text{for} \quad R_1^2/R_2 < |z| < R_1 \tag{17}$$

$$\mathbf{f}_{2**}(z) = -\overline{\mathbf{f}_2}(R_2^2/z) \quad \text{for} \quad R_2 < |z| < R_2^2/R_1 \tag{18}$$

$$\mathbf{f}_{3*}(z) = -\overline{\mathbf{f}_3}(R_2^2/z) \quad \text{for} \quad |z| < R_2 \tag{19}$$

where the overbar represents the complex conjugate.

3. Piezoelectric screw dislocation inside the matrix

Let us first analyze the singularities of the complex function vectors. If a piezoelectric dislocation is located in the matrix, referring to Pak (1990) and Liu et al. (2000), the generalized analytical function vector $\mathbf{f}_3(z)$ in the matrix can be chosen as:

$$\mathbf{f}_3(z) = \frac{1}{2\pi \mathrm{i}}\mathbf{b}\ln(z - z_0) + \mathbf{f}_{30}(z) \quad |z| > R_2 \tag{20}$$

where the first term represents the complex potential for a piezoelectric screw dislocation in an infinite matrix in the absence of the inclusion; the second term represents the disturbance of the complex potential due to the presence of a circular inclusion and an interphase layer. The second term $\mathbf{f}_{30}(z)$ is holomorphic in the region $|z| > R_2$. From Eq. (19), it is seen that

$$\mathbf{f}_{3*}(z) = \frac{1}{2\pi \mathrm{i}}\mathbf{b}\ln\left(\frac{R_2^2}{z} - \overline{z_0}\right) + \mathbf{f}_{3*0}(z) \quad |z| < R_2 \tag{21}$$

where $\mathbf{f}_{3*0}(z)$ is holomorphic in the defined region.

Neglecting the constant terms denoting the rigid displacement and equipotential field, function vector $\mathbf{f}_2(z)$ can be expanded into Laurent series in the annular region:

$$\mathbf{f}_2(z) = \mathbf{G}_N(z) + \mathbf{G}_P(z) \quad \text{for} \quad R_1 < |z| < R_2 \tag{22}$$

with $\mathbf{G}_N(z) = \sum_{k=0}^{\infty} \mathbf{a}_k z^{-(k+1)}$ and $\mathbf{G}_P(z) = \sum_{k=0}^{\infty} \mathbf{b}_k z^{k+1}$.

The substitution of Eq. (22) into Eqs. (17) and (18) yields:

$$\mathbf{f}_{2*}(z) = -\overline{\mathbf{G}_N}(R_1^2/z) - \overline{\mathbf{G}_P}(R_1^2/z) \quad \text{for} \quad R_1^2/R_2 < |z| < R_1 \tag{23}$$

$$\mathbf{f}_{2**}(z) = -\overline{\mathbf{G}_N}(R_2^2/z) - \overline{\mathbf{G}_P}(R_2^2/z) \quad \text{for} \quad R_2 < |z| < R_2^2/R_1 \tag{24}$$

Obviously, $\mathbf{f}_1(z)$ is holomorphic in the region $|z| < R_1$, and from Eq. (16), $\mathbf{f}_{1*}(z)$ is holomorphic in the defined region.

The substitution of Eq. (13) into the first equation of Eqs. (14) and (15) yields:

$$M_1\lfloor\overline{\mathbf{f}_1(t)} - \mathbf{f}_1(t)\rfloor = M_2\lfloor\overline{\mathbf{f}_2(t)} - \mathbf{f}_2(t)\rfloor \quad \text{on } |t| = R_1 \tag{25}$$

$$M_2\lfloor\overline{\mathbf{f}_2(t)} - \mathbf{f}_2(t)\rfloor = M_3\lfloor\overline{\mathbf{f}_3(t)} - \mathbf{f}_3(t)\rfloor \quad \text{on } |t| = R_2 \tag{26}$$

Noting that $\overline{t}t = R_1^2$ on $|t| = R_1$ and $\overline{t}t = R_2^2$ on $|t| = R_2$, and using Eqs. (16)–(19), Eqs. (25) and (26) can be rewritten as:

$$[M_2\mathbf{f}_{2*}(t) - M_1\mathbf{f}_1(t) + M_3\mathbf{f}_{3*}(t)]^{\mathrm{I}} = [M_1\mathbf{f}_{1*}(t) - M_2\mathbf{f}_2(t) + M_3\mathbf{f}_{3*}(t)]^{\mathrm{L}} \quad \text{on } |t| = R_1 \tag{27}$$

$$[M_1\mathbf{f}_{1*}(t) - M_2\mathbf{f}_2(t) + M_3\mathbf{f}_{3*}(t)]^{\mathrm{L}} = [M_2\mathbf{f}_{2**}(t) - M_3\mathbf{f}_3(t) + M_1\mathbf{f}_{1*}(t)]^{\mathrm{M}} \quad \text{on } |t| = R_2 \tag{28}$$

where the superscript I, L and M refer to the function value as approached from the regions occupied by the inclusion, the interphase layer and the matrix, respectively. Eqs. (27) and (28) imply that $[M_2\mathbf{f}_{2*}(z) - M_1\mathbf{f}_1(z) + M_3\mathbf{f}_{3*}(z)]$, $[M_1\mathbf{f}_{1*}(z) - M_2\mathbf{f}_2(z) + M_3\mathbf{f}_{3*}(z)]$ and $[M_2\mathbf{f}_{2**}(z) - M_3\mathbf{f}_3(z) + M_1\mathbf{f}_{1*}(z)]$ are the mutual direct analytical continuation, and they can be expressed by a continuous function vector $\mathbf{f}_T(z)$:

$$\mathbf{f}_T(z) = \begin{cases} M_2\mathbf{f}_{2*}(z) - M_1\mathbf{f}_1(z) + M_3\mathbf{f}_{3*}(z) & R_1^2/R_2 < |z| < R_1 \\ M_1\mathbf{f}_{1*}(z) - M_2\mathbf{f}_2(z) + M_3\mathbf{f}_{3*}(z) & R_1 < |z| < R_2 \\ M_2\mathbf{f}_{2**}(z) - M_3\mathbf{f}_3(z) + M_1\mathbf{f}_{1*}(z) & R_2 < |z| < R_2^2/R_1 \end{cases} \tag{29}$$

Similarly, substituting Eq. (8) into the second equation of Eqs. (14) and (15) and considering Eqs. (16)–(19), we obtain the expression of continuous function vector $\mathbf{f}_U(z)$:

$$\mathbf{f}_U(z) = \begin{cases} \mathbf{f}_1(z) + \mathbf{f}_{2*}(z) + \mathbf{f}_{3*}(z) & R_1^2/R_2 < |z| < R_1 \\ \mathbf{f}_{1*}(z) + \mathbf{f}_2(z) + \mathbf{f}_{3*}(z) & R_1 < |z| < R_2 \\ \mathbf{f}_{1*}(z) + \mathbf{f}_{2**}(z) + \mathbf{f}_3(z) & R_2 < |z| < R_2^2/R_1 \end{cases} \tag{30}$$

Noting Eqs. (29) and (30) and defining

$$\mathbf{f}_T(z) = \begin{cases} M_3\mathbf{f}_{3*}(z) - M_1\mathbf{f}_1(z) & |z| < R_1^2/R_2 \\ M_1\mathbf{f}_{1*}(z) - M_3\mathbf{f}_3(z) & |z| > R_2^2/R_1 \end{cases} \tag{31}$$

$$\mathbf{f}_U(z) = \begin{cases} \mathbf{f}_1(z) + \mathbf{f}_{3*}(z) & |z| < R_1^2/R_2 \\ \mathbf{f}_{1*}(z) + \mathbf{f}_3(z) & |z| > R_2^2/R_1 \end{cases} \tag{32}$$

where $\mathbf{f}_T(z)$ and $\mathbf{f}_U(z)$ are two sectional analytical function vectors with the contours as shown in Fig. 2 and the boundary conditions:

$$\mathbf{f}_T^+(t) - \mathbf{f}_T^-(t) = \begin{cases} M_2\mathbf{f}_{2*}(t) & |t| = R_1^2/R_2 \\ M_2\mathbf{f}_{2**}(t) & |t| = R_2^2/R_1 \end{cases} \tag{33}$$

$$\mathbf{f}_U^+(t) - \mathbf{f}_U^-(t) = \begin{cases} \mathbf{f}_{2*}(t) & |t| = R_1^2/R_2 \\ \mathbf{f}_{2**}(t) & |t| = R_2^2/R_1 \end{cases} \tag{34}$$

where the superscript + and − represent the function vectors boundary values as approached from regions S^+ and S^-, respectively, as shown in Fig. 2.

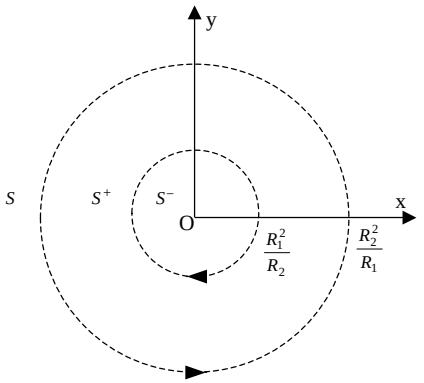

Fig. 2. Internal boundaries for the sectional analytical function vectors.

Now the problem is reduced to the boundary value problem of two sectionally analytical function vectors $\mathbf{f}_T(z)$ and $\mathbf{f}_U(z)$.

By using Eqs. (20)–(24), Eqs. (33) and (34) can be expressed as follows:

$$\mathbf{f}^+_{T0}(t)-\mathbf{f}^-_{T0}(t)=\begin{cases}-M_2[\overline{\mathbf{G}_N}(R_1^2/t)+\overline{\mathbf{G}_P}(R_1^2/t)]+M_3\mathbf{B}\ln(R_2^2/t-\overline{z_0}) & |t|=R_1^2/R_2\\ -M_2[\overline{\mathbf{G}_N}(R_2^2/t)+\overline{\mathbf{G}_P}(R_2^2/t)]-M_3\mathbf{B}\ln(t-z_0) & |t|=R_2^2/R_1\end{cases} \tag{35}$$

and

$$\mathbf{f}^+_{U0}(t)-\mathbf{f}^-_{U0}(t)=\begin{cases}-[\overline{\mathbf{G}_N}(R_1^2/t)+\overline{\mathbf{G}_P}(R_1^2/t)]+\mathbf{B}\ln(R_2^2/t-\overline{z_0}) & |t|=R_1^2/R_2\\ -[\overline{\mathbf{G}_N}(R_2^2/t)+\overline{\mathbf{G}_P}(R_2^2/t)]+\mathbf{B}\ln(t-z_0) & |t|=R_2^2/R_1\end{cases} \tag{36}$$

where $\mathbf{B}=\frac{1}{2\pi\mathrm{i}}\mathbf{b}=\frac{1}{2\pi\mathrm{i}}\begin{Bmatrix}b_z\\ b_\varphi\end{Bmatrix}$.

From Eq. (35), $\mathbf{f}_{T0}(z)$ can be represented by the Cauchy integrals:

$$\begin{aligned}\mathbf{f}_{T0}(z)=&\frac{1}{2\pi\mathrm{i}}\int_{|t|=R_1^2/R_2}\frac{-M_2[\overline{\mathbf{G}_N}(R_1^2/t)+\overline{\mathbf{G}_P}(R_1^2/t)]+M_3\mathbf{B}\ln(R_2^2/t-\overline{z_0})}{t-z}\,\mathrm{d}t\\&+\frac{1}{2\pi\mathrm{i}}\int_{|t|=R_2^2/R_1}\frac{-M_2[\overline{\mathbf{G}_N}(R_2^2/t)+\overline{\mathbf{G}_P}(R_2^2/t)]-M_3\mathbf{B}\ln(t-z_0)}{t-z}\,\mathrm{d}t\end{aligned} \tag{37}$$

where the integration contours for the above Cauchy integrals are shown in Fig. 2.

According to Muskhelishvili (1975), Cauchy integrals on the right hand side of Eq. (35) can be integrated in closed form:

$$\mathbf{f}_{T0}(z)=M_3\mathbf{f}_{3*0}(z)-M_1\mathbf{f}_1(z)=M_2\overline{\mathbf{G}_N}(R_1^2/z)-M_2\overline{\mathbf{G}_N}(R_2^2/z)-M_3\mathbf{B}\ln(z-z_0)\quad |z|<R_1^2/R_2 \tag{38}$$

$$\begin{aligned}\mathbf{f}_{T0}(z)&=M_2\mathbf{f}_{2*}(z)-M_1\mathbf{f}_1(z)+M_3\mathbf{f}_{3*}(z)=M_1\mathbf{f}_{1*}(z)-M_2\mathbf{f}_2(z)+M_3\mathbf{f}_{3*}(z)\\&=M_2\mathbf{f}_{2**}(z)-M_3\mathbf{f}_3(z)+M_1\mathbf{f}_{1*}(z)\\&=-M_2\overline{\mathbf{G}_P}(R_1^2/z)+M_3\mathbf{B}\ln(R_2^2/z-\overline{z_0})-M_2\overline{\mathbf{G}_N}(R_2^2/z)-M_3\mathbf{B}\ln(z-z_0)\quad R_1^2/R_2<|z|<R_2^2/R_1\end{aligned} \tag{39}$$

$$\mathbf{f}_{T0}(z)=M_1\mathbf{f}_{1*}(z)-M_3\mathbf{f}_{30}(z)=-M_2\overline{\mathbf{G}_P}(R_1^2/z)+M_2\overline{\mathbf{G}_P}(R_2^2/z)+M_3\mathbf{B}\ln(R_2^2/z-\overline{z_0})\quad |z|>R_2^2/R_1 \tag{40}$$

Similarly, Eq. (36) leads to

$$\begin{aligned}\mathbf{f}_{U0}(z)=&\frac{1}{2\pi\mathrm{i}}\int_{|t|=R_1^2/R_2}\frac{-[\overline{\mathbf{G}_N}(R_1^2/t)+\overline{\mathbf{G}_P}(R_1^2/t)]+\mathbf{B}\ln(R_2^2/t-\overline{z_0})}{t-z}\,\mathrm{d}t\\&+\frac{1}{2\pi\mathrm{i}}\int_{|t|=R_2^2/R_1}\frac{-[\overline{\mathbf{G}_N}(R_2^2/t)+\overline{\mathbf{G}_P}(R_2^2/t)]+\mathbf{B}\ln(t-z_0)}{t-z}\,\mathrm{d}t\end{aligned} \tag{41}$$

Further,

$$\mathbf{f}_{U0}(z)=\mathbf{f}_{3*0}(z)+\mathbf{f}_1(z)=\overline{\mathbf{G}_N}(R_1^2/z)-\overline{\mathbf{G}_N}(R_2^2/z)+\mathbf{B}\ln(z-z_0)\quad |z|<R_1^2/R_2 \tag{42}$$

$$\begin{aligned}\mathbf{f}_{U0}(z)&=\mathbf{f}_{2*}(z)+\mathbf{f}_1(z)+\mathbf{f}_{3*}(z)=\mathbf{f}_{1*}(z)+\mathbf{f}_2(z)+\mathbf{f}_{3*}(z)=\mathbf{f}_{2**}(z)+\mathbf{f}_3(z)+\mathbf{f}_{1*}(z)\\&=-\overline{\mathbf{G}_P}(R_1^2/z)+\mathbf{B}\ln(R_2^2/z-\overline{z_0})-\overline{\mathbf{G}_N}(R_2^2/z)+\mathbf{B}\ln(z-z_0)\quad R_1^2/R_2<|z|<R_2^2/R_1\end{aligned} \tag{43}$$

$$\mathbf{f}_{U0}(z)=\mathbf{f}_{1*}(z)+\mathbf{f}_{30}(z)=-\overline{\mathbf{G}_P}(R_1^2/z)+\overline{\mathbf{G}_P}(R_2^2/z)+\mathbf{B}\ln(R_2^2/z-\overline{z_0})\quad |z|>R_2^2/R_1 \tag{44}$$

From Eqs. (38) and (42), it is seen that

$$\begin{aligned}\mathbf{f}_1(z) &= 2[M_1+M_3]^{-1}M_3\mathbf{B}\ln(z-z_0)+[M_1+M_3]^{-1}[M_3-M_2]\overline{\mathbf{G}_N}(R_1^2/z)\\ &\quad+[M_1+M_3]^{-1}[M_2-M_3]\overline{\mathbf{G}_N}(R_2^2/z)\quad |z|<R_1\end{aligned}\tag{45}$$

From Eqs. (40) and (44), it is seen that

$$\begin{aligned}\mathbf{f}_3(z) &= \mathbf{B}\ln(z-z_0)+[M_1+M_3]^{-1}[M_1-M_3]\mathbf{B}\ln(R_2^2/z-\overline{z_0})+[M_1+M_3]^{-1}[M_2-M_1]\overline{\mathbf{G}_P}(R_1^2/z)\\ &\quad+[M_1+M_3]^{-1}[M_1-M_2]\overline{\mathbf{G}_P}(R_2^2/z)\quad |z|>R_2\end{aligned}\tag{46}$$

where superscript -1 denotes the inverse of the matrix.

Eqs. (45) and (46) show that both complex potential $\mathbf{f}_1(z)$ and $\mathbf{f}_3(z)$ are related to the complex potential $\mathbf{f}_2(z)=\mathbf{G}_N(z)+\mathbf{G}_P(z)$. The remaining task is to determine the complex function vector $\mathbf{f}_2(z)$. From Eqs. (39) and (43), the following equation can be derived:

$$\begin{aligned}&\{[M_3-M_1][M_1+M_3]^{-1}[M_1-M_2]+[M_1+M_2]\}\mathbf{G}_P(z)+[M_1+M_2]\mathbf{G}_N(z)\\ &\quad+[M_3-M_1][M_1+M_3]^{-1}[M_2-M_1]\mathbf{G}_P\left(\frac{R_1^2}{R_2^2}z\right)+[M_1-M_2]\overline{\mathbf{G}_P}\left(\frac{R_1^2}{z}\right)+[M_1-M_2]\overline{\mathbf{G}_N}\left(\frac{R_2^2}{z}\right)\\ &=\{[M_3-M_1][M_1+M_3]^{-1}[M_1-M_3]+[M_1+M_3]\}\mathbf{B}\ln(z-z_0)\end{aligned}\tag{47}$$

Noting that

$$\ln(z-z_0)=\ln(-z_0)-\sum_{k=0}^{\infty}\frac{1}{k+1}\left(\frac{z}{z_0}\right)^{k+1}\quad |z|<|z_0|\tag{48}$$

Neglecting the constant terms representing the rigid displacement and equipotential field, the substituting Eq. (22) into Eq. (47) and comparison of the coefficient of the same power terms yields:

$$[M_1+M_2]\mathbf{a}_k+[M_1-M_2]\overline{\mathbf{b}_k}R_1^{2(k+1)}=0\tag{49}$$

$$\begin{aligned}&\{[M_3-M_1][M_1+M_3]^{-1}[M_1-M_2]+[M_1+M_2]\}\mathbf{b}_k\\ &\quad+[M_3-M_1][M_1+M_3]^{-1}[M_2-M_1]\mathbf{b}_k\left(\frac{R_1}{R_2}\right)^{2(k+1)}+[M_1-M_2]\overline{\mathbf{a}_k}R_2^{-2(k+1)}\\ &=-\{[M_3-M_1][M_1+M_3]^{-1}[M_1-M_3]+[M_1+M_3]\}\mathbf{B}\frac{1}{k+1}z_0^{-(k+1)}\end{aligned}\tag{50}$$

From Eqs. (47) and (48), the explicit expressions of the coefficients $\mathbf{a}_k$ and $\mathbf{b}_k$ are easy to obtain

$$\mathbf{a}_k=[M_1+M_2]^{-1}[M_1-M_2]\Pi^{-1}\Omega\mathbf{b}\frac{1}{2\pi\mathrm{i}(k+1)}\left(\frac{R_1^2}{\overline{z_0}}\right)^{k+1}\tag{51}$$

$$\mathbf{b}_k=\Pi^{-1}\Omega\mathbf{b}\frac{1}{2\pi\mathrm{i}(k+1)}z_0^{-(k+1)}\tag{52}$$

where

$$\begin{aligned}\Pi &= \{[M_3-M_1][M_1+M_3]^{-1}[M_1-M_2]+[M_1+M_2]\}R_2^{2(k+1)}+[M_3-M_1][M_1+M_3]^{-1}[M_2-M_1]R_1^{2(k+1)}\\ &\quad+[M_2-M_1][M_1+M_2]^{-1}[M_1-M_2]R_1^{2(k+1)}\end{aligned}$$

and,

$$\Omega = \{[M_1 - M_3][M_1 + M_3]^{-1}[M_1 - M_3] - [M_1 + M_3]\}R_2^{2(k+1)}$$

Now the complex function vectors $\mathbf{f}_1(z)$, $\mathbf{f}_2(z)$ and $\mathbf{f}_3(z)$ have been determined by Eqs. (45), (22) and (46). The electroelastic field variables in the inclusion and the matrix can be evaluated by means of Eqs. (11) and (12).

As the special case, the solutions for a circular inclusion in the infinite matrix can be obtained by letting $M_1 = M_2$ in Eqs. (45), (22) and (46):

$$\mathbf{f}_1(z) = \mathbf{f}_2(z) = \frac{1}{\pi \mathrm{i}}[M_1 + M_3]^{-1}M_3\mathbf{b}\ln(z - z_0) \tag{53}$$

$$\mathbf{f}_3(z) = \frac{1}{2\pi \mathrm{i}}\mathbf{b}\ln(z - z_0) + \frac{1}{2\pi \mathrm{i}}[M_1 + M_3]^{-1}[M_1 - M_3]\mathbf{b}\ln(R_2^2/z - \overline{z_0}) \tag{54}$$

Eqs. (53) and (54) are identical to the results in Kattis et al. (1998) and Liu et al. (2000).

4. Piezoelectric screw dislocation inside the inclusion

For a screw dislocation located at the point $z = z_0$ inside the inclusion, the complex function vectors can be written as:

$$\mathbf{f}_1(z) = \frac{1}{2\pi \mathrm{i}}\mathbf{b}\ln(z - z_0) + \mathbf{f}_{10}(z) \quad |z| < R_1 \tag{55}$$

$$\mathbf{f}_2(z) = \frac{1}{2\pi \mathrm{i}}\mathbf{b}\ln(z - z_0) + \mathbf{f}_{20}(z) \quad R_1 < |z| < R_2 \tag{56}$$

$$\mathbf{f}_3(z) = \frac{1}{2\pi \mathrm{i}}\mathbf{b}\ln(z - z_0) + \mathbf{f}_{30}(z) \quad |z| > R_2 \tag{57}$$

where the complex function vectors $\mathbf{f}_{10}(z)$, $\mathbf{f}_{20}(z)$ and $\mathbf{f}_{30}(z)$ are holomorphic in the regions where they are defined, respectively. $\mathbf{f}_{20}(z)$ can be expanded into Laurent series:

$$\mathbf{f}_{20}(z) = \mathbf{G}_N(z) + \mathbf{G}_P(z) \quad \text{for} \quad R_1 < |z| < R_2 \tag{58}$$

with $\mathbf{G}_N(z) = \sum_{k=0}^{\infty}\mathbf{a}'_k z^{-(k+1)}$ and $\mathbf{G}_P(z) = \sum_{k=0}^{\infty}\mathbf{b}'_k z^{k+1}$.

Referring to Eqs. (16)–(19), the four introduced complex function vectors can be written as:

$$\mathbf{f}_{1*}(z) = \frac{1}{2\pi \mathrm{i}}\mathbf{b}\ln\left(\frac{R_1}{z} - \overline{z_0}\right) + \mathbf{f}_{1*0}(z) \quad |z| > R_1 \tag{59}$$

$$\mathbf{f}_{2*}(z) = \frac{1}{2\pi \mathrm{i}}\mathbf{b}\ln\left(\frac{R_1}{z} - \overline{z_0}\right) - \overline{\mathbf{G}_N}(R_1^2/z) - \overline{\mathbf{G}_P}(R_1^2/z) \quad R_1^2/R_2 < |z| < R_1 \tag{60}$$

$$\mathbf{f}_{2**}(z) = \frac{1}{2\pi \mathrm{i}}\mathbf{b}\ln\left(\frac{R_2}{z} - \overline{z_0}\right) - \overline{\mathbf{G}_N}(R_2^2/z) - \overline{\mathbf{G}_P}(R_2^2/z) \quad R_2 < |z| < R_2^2/R_1 \tag{61}$$

$$\mathbf{f}_{3*}(z) = \frac{1}{2\pi \mathrm{i}}\mathbf{b}\ln\left(\frac{R_2}{z} - \overline{z_0}\right) + \mathbf{f}_{3*0}(z) \quad |z| < R_2 \tag{62}$$

Using the similar method in the above section, the relations of the complex potentials $\mathbf{f}_1(z)$ and $\mathbf{f}_3(z)$ with the complex potential $\mathbf{f}_2(z)$ can be obtained:

$$\begin{aligned}\mathbf{f}_1(z) &= \mathbf{B}\ln(z-z_0) + [M_1+M_3]^{-1}[M_2-M_1]\mathbf{B}\ln(z-R_1^2/\overline{z_0}) + [M_1+M_3]^{-1}[M_3-M_2]\mathbf{B}\ln(z-R_2^2/\overline{z_0}) \\ &\quad + [M_1+M_3]^{-1}[M_3-M_2]\overline{\mathbf{G}_N}(R_1^2/z) + [M_1+M_3]^{-1}[M_2-M_3]\overline{\mathbf{G}_N}(R_2^2/z) \quad |z|<R_1 \end{aligned} \tag{63}$$

$$\begin{aligned}\mathbf{f}_3(z) &= 2[M_1+M_3]^{-1}M_1\mathbf{B}\ln(z-z_0) + [M_1+M_3]^{-1}[M_3-M_1]\mathbf{B}\ln z + [M_1+M_3]^{-1}[M_2-M_1]\overline{\mathbf{G}_P}(R_1^2/z) \\ &\quad + [M_1+M_3]^{-1}[M_1-M_2]\overline{\mathbf{G}_P}(R_2^2/z) \quad |z|>R_2 \end{aligned} \tag{64}$$

The complex potential $\mathbf{f}_{20}(z) = \mathbf{G}_N(z) + \mathbf{G}_P(z)$ is determined by the following equations:

$$\begin{aligned}&\{[M_3-M_1][M_1+M_3]^{-1}[M_1-M_2]+[M_1+M_2]\} + [M_3-M_1][M_1+M_3]^{-1}[M_2-M_1]\mathbf{G}_P\left(\frac{R_1^2}{R_2^2}z\right) \\ &\quad + [M_1+M_2]\mathbf{G}_N(z) + [M_1-M_2]\overline{\mathbf{G}_P}\left(\frac{R_1^2}{z}\right) + [M_1-M_2]\overline{\mathbf{G}_N}\left(\frac{R_2^2}{z}\right) \\ &= [M_1-M_2]\mathbf{B}\ln\left(1-\frac{z_0}{z}\right) + \{2[M_3-M_1][M_1+M_3]^{-1}M_1 + M_1 - M_2\}\mathbf{B}\ln\left(1-\frac{z\overline{z_0}}{R_2^2}\right) \end{aligned} \tag{65}$$

Noting that

$$\ln\left(1-\frac{z\overline{z_0}}{R_2^2}\right) = -\sum_{k=0}^{\infty}\frac{1}{k+1}\left(\frac{z\overline{z_0}}{R_2^2}\right)^{k+1} \quad \text{for} \quad |z| < \left|\frac{R_2^2}{\overline{z_0}}\right| \tag{66}$$

and

$$\ln\left(1-\frac{z_0}{z}\right) = -\sum_{k=0}^{\infty}\frac{1}{k+1}\left(\frac{z_0}{z}\right)^{k+1} \quad \text{for} \quad |z| > |z_0| \tag{67}$$

The substituting Eqs. (66), (67) and (59) into Eq. (65), and comparison of the coefficient of the same power terms yields:

$$\begin{aligned}\mathbf{a}_k' &= [M_1+M_2]^{-1}[M_2-M_1]\mathbf{b}\frac{1}{2\pi\mathrm{i}(k+1)}z_0^{(k+1)} \\ &\quad + [M_1+M_2]^{-1}[M_1-M_2]\Pi'^{-1}\Omega'\mathbf{b}\frac{1}{2\pi\mathrm{i}(k+1)}z_0^{(k+1)}\left(\frac{R_1}{R_2}\right)^{2(k+1)} \end{aligned} \tag{68}$$

$$\mathbf{b}_k' = \Pi'^{-1}\Omega'\mathbf{b}\frac{1}{2\pi\mathrm{i}(k+1)}\left(\frac{\overline{z_0}}{R_2^2}\right)^{k+1} \tag{69}$$

where

$$\begin{aligned}\Pi' &= \{[M_3-M_1][M_1+M_3]^{-1}[M_1-M_2]+[M_1+M_2]\} + [M_3-M_1][M_1+M_3]^{-1}[M_2-M_1]\left(\frac{R_1}{R_2}\right)^{2(k+1)} \\ &\quad + [M_1-M_2][M_1+M_2]^{-1}[M_2-M_1]\left(\frac{R_1}{R_2}\right)^{2(k+1)} \end{aligned}$$

and

$$\Omega' = [M_2-M_1][M_1+M_2]^{-1}[M_1-M_2] + 2[M_1-M_3][M_1+M_3]^{-1}M_1 - M_1 + M_2$$

Now the complex function vectors $\mathbf{f}_1(z)$, $\mathbf{f}_2(z)$ and $\mathbf{f}_3(z)$ have been determined by Eqs. (63), (58) and (64).

At this point two special cases for the problem will be considered.

(a) Assuming $M_3 = 0$, Eqs. (68) and (69) will be reduced to the solutions on the interaction between a piezoelectric screw dislocation and a coated cylinder. In this case, Π' and Ω' can be expressed as follow:

$$\Pi' = 2M_2 + \{[M_1 - M_2][M_1 + M_2]^{-1}[M_2 - M_1] + M_1 - M_2\}\left(\frac{R_1}{R_2}\right)^{2(k+1)} \tag{70}$$

$$\Omega' = [M_2 - M_1][M_1 + M_2]^{-1}[M_1 - M_2] + M_1 + M_2 \tag{71}$$

(b) The solutions for a circular piezoelectric inclusion in the infinite piezoelectric matrix can be obtained by letting $M_2 = M_3$ (or $M_1 = M_2$) in Eqs. (63), (22) and (64):

$$\mathbf{f}_1(z) = \frac{1}{2\pi \mathrm{i}}\mathbf{b}\ln(z - z_0) + \frac{1}{2\pi \mathrm{i}}[M_1 + M_3]^{-1}[M_2 - M_1]\mathbf{b}\ln(z - R_1^2/\overline{z_0}) \tag{72}$$

$$\mathbf{f}_3(z) = \frac{1}{2\pi \mathrm{i}}[M_1 + M_3]^{-1}M_1\mathbf{b}\ln(z - z_0) + \frac{1}{2\pi \mathrm{i}}[M_1 + M_3]^{-1}[M_3 - M_1]\mathbf{b}\ln z \tag{73}$$

In the absence of the piezoelectric coupling effect, the results of Eqs. (72) and (73) are identical to those of Smith (1968).

5. Image force on the dislocation

The image force (Hirth and Lothe, 1982) on the dislocation is an important physical parameter in understanding electroelastic behavior of inhomogeneous material, especially in understanding the mobility and so-called trapping mechanism of the dislocation. Additionally, it can be used to study the crack growth in composites, as well as strengthening and hardening mechanisms in alloyed materials. The image force can be evaluated by means of the generalized Peach–Koehler formula by Pak (1990).

$$F_x - \mathrm{i}F_y = \mathrm{i}\mathbf{b}^{\mathrm{T}}(\boldsymbol{\Sigma}_x^0 - \mathrm{i}\boldsymbol{\Sigma}_y^0) \tag{74}$$

where $\boldsymbol{\Sigma}_x^0$ and $\boldsymbol{\Sigma}_y^0$ denote the perturbation stress and electric displacement components at the dislocation point.

Referring to the work by Qaissaunee and Santare (1995), we have

$$\begin{aligned}\boldsymbol{\Sigma}_x^0 - \mathrm{i}\boldsymbol{\Sigma}_y^0 &= \frac{1}{2\pi \mathrm{i}}M_3[M_1 + M_3]^{-1}[M_1 - M_3]\mathbf{b}\left(\frac{1}{z_0 - R_2^2/\overline{z_0}} - \frac{1}{z_0}\right) + \frac{1}{2\pi \mathrm{i}}\sum_{k=0}^{\infty} M_3[M_1 + M_3]^{-1}[M_2 - M_1]\Pi^{-1}\Omega\mathbf{b}\frac{R_1^{2(k+1)}}{\overline{z_0}^{k+1}z_0^{k+2}} \\ &\quad + \frac{1}{2\pi \mathrm{i}}\sum_{k=0}^{\infty} M_3[M_1 + M_3]^{-1}[M_1 - M_2]\Pi^{-1}\Omega b\frac{R_2^{2(k+1)}}{\overline{z_0}^{k+1}z_0^{k+2}}\end{aligned} \tag{75}$$

for the dislocation in the matrix, and

$$\begin{aligned}\boldsymbol{\Sigma}_x^0 - \mathrm{i}\boldsymbol{\Sigma}_y^0 = {} & \frac{1}{2\pi\mathrm{i}} M_1[M_1+M_3]^{-1}[M_2-M_1]\mathbf{b}\frac{1}{z_0-R_1^2/\overline{z_0}} + \frac{1}{2\pi\mathrm{i}} M_1[M_1+M_3]^{-1}[M_3-M_2]\mathbf{b}\frac{1}{z_0-R_2^2/\overline{z_0}} \\ & + \frac{1}{2\pi\mathrm{i}}\sum_{k=0}^{\infty} M_1[M_1+M_3]^{-1}[M_3-M_2][M_1+M_2]^{-1}[M_1-M_2]\mathbf{b}\frac{z_0^k\overline{z_0}^{k+1}}{R_1^{2k+2}} \\ & + \frac{1}{2\pi\mathrm{i}}\sum_{k=0}^{\infty} M_1[M_1+M_3]^{-1}[M_3-M_2][M_1+M_2]^{-1}[M_2-M_1]\Pi'^{-1}\Omega'\mathbf{b}\frac{z_0^k\overline{z_0}^{k+1}}{R_2^{2k+2}} \\ & + \frac{1}{2\pi\mathrm{i}}\sum_{k=0}^{\infty} M_1[M_1+M_3]^{-1}[M_2-M_3][M_1+M_2]^{-1}[M_1-M_2]\mathbf{b}\frac{z_0^k\overline{z_0}^{k+1}}{R_2^{2k+2}} \\ & + \frac{1}{2\pi\mathrm{i}}\sum_{k=0}^{\infty} M_1[M_1+M_3]^{-1}[M_2-M_3][M_1+M_2]^{-1}[M_2-M_1]\Pi'^{-1}\Omega'\mathbf{b}\frac{z_0^k\overline{z_0}^{k+1}}{R_1^{2(k+1)}}R_2^{2(2k+2)}\end{aligned} \tag{76}$$

for the dislocation in the inclusion.

The substitution of Eqs. (75) and (76) into Eq. (74), the explicit expressions of the image force on the piezoelectric screw dislocation can be obtained.

6. Examples and discussions

In this section, three examples are given to illustrate the influence of the interphase layer parameters on the image force.

6.1. Three-phase elastic–dielectric inclusion

In this case, let us assume that piezoelectric constants within the inclusion, the interphase layer and the matrix are zero, respectively (i.e. $e_{15}^{(1)} = e_{15}^{(2)} = e_{15}^{(3)} = 0$, where and hereafter the superscripts 1, 2 and 3 represent the inclusion, the interphase layer and the matrix, respectively).

Assuming the piezoelectric screw dislocation is located at the point z_0 in the matrix, from Eqs. (74) and (75), one obtains

$$\begin{aligned}F_x - \mathrm{i}F_y = {} & \frac{C_{44}^{(3)}b_z^2}{2\pi}\left\{\frac{C_{44}^{(1)}-C_{44}^{(3)}}{C_{44}^{(1)}+C_{44}^{(3)}}\left(\frac{1}{z_0-R_2^2/\overline{z_0}}-\frac{1}{z_0}\right)+\left[\frac{\left(C_{44}^{(1)}-C_{44}^{(2)}\right)R_1^{2k+2}}{C_{44}^{(1)}+C_{44}^{(3)}}+\frac{\left(C_{44}^{(2)}-C_{44}^{(1)}\right)R_2^{2k+2}}{C_{44}^{(1)}+C_{44}^{(3)}}\right]\right. \\ & \left.\times\frac{2C_{44}^{(3)}\left(C_{44}^{(1)}+C_{44}^{(3)}\right)}{\left(C_{44}^{(2)}+C_{44}^{(3)}\right)\left(C_{44}^{(1)}+C_{44}^{(2)}\right)+\left(C_{44}^{(3)}-C_{44}^{(2)}\right)\left(C_{44}^{(2)}-C_{44}^{(1)}\right)(R_1/R_2)^{2k+2}}\frac{1}{\overline{z_0}^{k+1}z_0^{k+2}}\right\} \\ & + \frac{d_{11}^{(3)}b_\varphi^2}{2\pi}\left\{\frac{d_{11}^{(3)}-d_{11}^{(1)}}{d_{11}^{(1)}+d_{11}^{(3)}}\left(\frac{1}{z_0-R_2^2/\overline{z_0}}-\frac{1}{z_0}\right)+\left[\frac{\left(d_{11}^{(2)}-d_{11}^{(1)}\right)R_1^{2k+2}}{d_{11}^{(1)}+d_{11}^{(3)}}+\frac{\left(d_{11}^{(1)}-d_{11}^{(2)}\right)R_2^{2k+2}}{d_{11}^{(1)}+d_{11}^{(3)}}\right]\right. \\ & \left.\times\frac{2d_{11}^{(3)}\left(d_{11}^{(1)}+d_{11}^{(3)}\right)}{\left(d_{11}^{(2)}+d_{11}^{(3)}\right)\left(d_{11}^{(1)}+d_{11}^{(2)}\right)+\left(d_{11}^{(3)}-d_{11}^{(2)}\right)\left(d_{11}^{(2)}-d_{11}^{(1)}\right)(R_1/R_2)^{2k+2}}\frac{1}{\overline{z_0}^{k+1}z_0^{k+2}}\right\}\end{aligned} \tag{77}$$

When the dislocation lies on the x-axis ($z_0 = x_0$, $x_0 > R_2$), the expression of Eq. (77) reduces to

$$F_x = \frac{C_{44}^{(3)} b_z^2}{2\pi}\left\{ \frac{C_{44}^{(1)} - C_{44}^{(3)}}{C_{44}^{(1)} + C_{44}^{(3)}} \frac{R_2^2}{(x_0^2 - R_2^2)x_0} + \left[\frac{\left(C_{44}^{(1)} - C_{44}^{(2)}\right)R_1^{2k+2}}{C_{44}^{(1)} + C_{44}^{(3)}} + \frac{\left(C_{44}^{(2)} - C_{44}^{(1)}\right)R_2^{2k+2}}{C_{44}^{(1)} + C_{44}^{(3)}} \right] \right.$$

$$\left. \times \frac{2C_{44}^{(3)}\left(C_{44}^{(1)} + C_{44}^{(3)}\right)}{\left(C_{44}^{(2)} + C_{44}^{(3)}\right)\left(C_{44}^{(1)} + C_{44}^{(2)}\right) + \left(C_{44}^{(3)} - C_{44}^{(2)}\right)\left(C_{44}^{(2)} - C_{44}^{(1)}\right)(R_1/R_2)^{2k+2}} \frac{1}{x_0^{2k+3}} \right\}$$

$$+ \frac{d_{11}^{(3)} b_\varphi^2}{2\pi}\left\{ \frac{d_{11}^{(3)} - d_{11}^{(1)}}{d_{11}^{(1)} + d_{11}^{(3)}} \frac{R_2^2}{x_0(x_0^2 - R_2^2)} + \left[\frac{\left(d_{11}^{(2)} - d_{11}^{(1)}\right)R_1^{2k+2}}{d_{11}^{(1)} + d_{11}^{(3)}} + \frac{\left(d_{11}^{(1)} - d_{11}^{(2)}\right)R_2^{2k+2}}{d_{11}^{(1)} + d_{11}^{(3)}} \right] \right.$$

$$\left. \frac{2d_{11}^{(3)}\left(d_{11}^{(1)} + d_{11}^{(3)}\right)}{\left(d_{11}^{(2)} + d_{11}^{(3)}\right)\left(d_{11}^{(1)} + d_{11}^{(2)}\right) + \left(d_{11}^{(3)} - d_{11}^{(2)}\right)\left(d_{11}^{(2)} - d_{11}^{(1)}\right)(R_1/R_2)^{2k+2}} \frac{1}{x_0^{2k+3}} \right\} \tag{78}$$

$$F_y = 0 \tag{79}$$

Above Eqs. (78) and (79) indicate the image force component F_y equals to zero and the screw dislocation only moves along the x-axis when the dislocation lies on the x-axis. Further analyses imply that the interphase layer geometry may be the dominant factor of the image force if the elastic–dielectric interphase layer is extremely compliant or rigid. In addition, the location of the dislocation also has significant effect on it.

Here, we may consider another case of piezoelectric inclusion with elastic interphase layer and elastic matrix. Piezoelectric composites sensors are often designed in this configuration where a piezoelectric bar is embedded into a surrounding elastic matrix (Sudak, 2003a,b; Deng and Meguid, 1999). In this case, piezoelectric constants and dielectric constants of the interphase and the matrix are zero respectively (i.e. $e_{15}^{(2)} = e_{15}^{(3)} = 0$, $d_{11}^{(2)} = d_{11}^{(3)} = 0$). Because the most general case of the piezoelectric inclusion with the piezoelectric interphase layer and the piezoelectric matrix will be discussed in the next section, we omit the details of the effect of the interphase layer parameters on the image force.

6.2. Piezoelectric inclusion with piezoelectric inter-phase layer and matrix

In this most general case let us assume the piezoelectric screw dislocation is located at the point z_0 in the matrix or in the inclusion. From Eqs. (74)–(76), one obtains

$$F_x - \mathrm{i}F_y$$

$$= \frac{1}{2\pi}\mathbf{b}^{\mathrm{T}} M_3[M_1 + M_3]^{-1}[M_1 - M_3]\mathbf{b}\left(\frac{1}{z_0 - R_2^2/\overline{z_0}} - \frac{1}{z_0}\right) + \frac{1}{2\pi}\sum_{k=0}^{\infty}\mathbf{b}^{\mathrm{T}} M_3[M_1 + M_3]^{-1}[M_2 - M_1]\Pi^{-1}\Omega\mathbf{b}\frac{R_1^{2(k+1)}}{\overline{z_0}^{k+1} z_0^{k+2}}$$

$$+ \frac{1}{2\pi}\sum_{k=0}^{\infty}\mathbf{b}^{\mathrm{T}} M_3[M_1 + M_3]^{-1}[M_1 - M_2]\Pi^{-1}\Omega\mathbf{b}\frac{R_2^{2(k+1)}}{\overline{z_0}^{k+1} z_0^{k+2}} \tag{80}$$

for the dislocation inside the matrix, and

$$\begin{aligned}F_x - \mathrm{i}F_y = {} & \frac{1}{2\pi}\mathbf{b}^{\mathrm{T}}M_1[M_1+M_3]^{-1}[M_2-M_1]\mathbf{b}\frac{1}{z_0-R_1^2/\overline{z_0}} + \frac{1}{2\pi\mathrm{i}}\mathbf{b}^{\mathrm{T}}M_1[M_1+M_3]^{-1}[M_3-M_2]\mathbf{b}\frac{1}{z_0-R_2^2/\overline{z_0}} \\ & + \frac{1}{2\pi}\sum_{k=0}^{\infty}\mathbf{b}^{\mathrm{T}}M_1[M_1+M_3]^{-1}[M_3-M_2][M_1+M_2]^{-1}[M_1-M_2]\mathbf{b}\frac{z_0^k\overline{z}_0^{k+1}}{R_1^{2k+2}} \\ & + \frac{1}{2\pi}\sum_{k=0}^{\infty}\mathbf{b}^{\mathrm{T}}M_1[M_1+M_3]^{-1}[M_3-M_2][M_1+M_2]^{-1}[M_2-M_1]\Pi'^{-1}\Omega'\mathbf{b}\frac{z_0^k\overline{z}_0^{k+1}}{R_2^{2k+2}} \\ & + \frac{1}{2\pi}\sum_{k=0}^{\infty}\mathbf{b}^{\mathrm{T}}M_1[M_1+M_3]^{-1}[M_2-M_3][M_1+M_2]^{-1}[M_1-M_2]\mathbf{b}\frac{z_0^k\overline{z}_0^{k+1}}{R_2^{2k+2}} \\ & + \frac{1}{2\pi}\sum_{k=0}^{\infty}\mathbf{b}^{\mathrm{T}}M_1[M_1+M_3]^{-1}[M_2-M_3][M_1+M_2]^{-1}[M_2-M_1]\Pi'^{-1}\Omega'\mathbf{b}\frac{z_0^k\overline{z}_0^{k+1}R_1^{2(k+1)}}{R_2^{2(2k+2)}} \end{aligned} \tag{81}$$

for the dislocation inside the inclusion.

The corresponding image force on the dislocation for the problem of the interaction between a piezoelectric screw dislocation in the infinite matrix and the circular piezoelectric inclusion can be obtained from Eq. (80) which coincides with the result in Liu et al. (2000). Here we omit details for saving space.

If the dislocation lies on the x-axis ($z_0 = x_0$), the expressions of Eqs. (80) and (81) reduce to:

$$\begin{aligned}F_x = {} & \frac{1}{2\pi}\mathbf{b}^{\mathrm{T}}M_3[M_1+M_3]^{-1}[M_1-M_3]\mathbf{b}\left(\frac{R_2^2}{x_0(x_0^2-R_2^2)}\right) + \frac{1}{2\pi}\sum_{k=0}^{\infty}\mathbf{b}^{\mathrm{T}}M_3[M_1+M_3]^{-1}[M_2-M_1]\Pi^{-1}\Omega\mathbf{b}\frac{R_1^{2(k+1)}}{x_0^{2k+3}} \\ & + \frac{1}{2\pi}\sum_{k=0}^{\infty}\mathbf{b}^{\mathrm{T}}M_3[M_1+M_3]^{-1}[M_1-M_2]\Pi^{-1}\Omega\mathbf{b}\frac{R_2^{2(k+1)}}{x_0^{2k+3}} \end{aligned} \tag{82}$$

$$F_y = 0 \tag{83}$$

for the dislocation inside the matrix, and

$$\begin{aligned}F_x = {} & \frac{1}{2\pi}\mathbf{b}^{\mathrm{T}}M_1[M_1+M_3]^{-1}[M_2-M_1]\mathbf{b}\frac{x_0}{x_0^2-R_1^2} + \frac{1}{2\pi}\mathbf{b}^{\mathrm{T}}M_1[M_1+M_3]^{-1}[M_3-M_2]\mathbf{b}\frac{x_0}{x_0^2-R_2^2} \\ & + \frac{1}{2\pi}\sum_{k=0}^{\infty}\mathbf{b}^{\mathrm{T}}M_1[M_1+M_3]^{-1}[M_3-M_2][M_1+M_2]^{-1}[M_1-M_2]\mathbf{b}\frac{x_0^{2k+1}}{R_1^{2k+2}} \\ & + \frac{1}{2\pi}\sum_{k=0}^{\infty}\mathbf{b}^{\mathrm{T}}M_1[M_1+M_3]^{-1}[M_3-M_2][M_1+M_2]^{-1}[M_2-M_1]\Pi'^{-1}\Omega'\mathbf{b}\frac{x_0^{2k+1}}{R_2^{2k+2}} \\ & + \frac{1}{2\pi}\sum_{k=0}^{\infty}\mathbf{b}^{\mathrm{T}}M_1[M_1+M_3]^{-1}[M_2-M_3][M_1+M_2]^{-1}[M_1-M_2]\mathbf{b}\frac{x_0^{2k+1}}{R_2^{2k+2}} \\ & + \frac{1}{2\pi}\sum_{k=0}^{\infty}\mathbf{b}^{\mathrm{T}}M_1[M_1+M_3]^{-1}[M_2-M_3][M_1+M_2]^{-1}[M_2-M_1]\Pi'^{-1}\Omega'\mathbf{b}\frac{x_0^{2k+1}R_1^{2(k+1)}}{R_2^{2(2k+2)}} \end{aligned} \tag{84}$$

$$F_y = 0 \tag{85}$$

for the dislocation inside the inclusion.

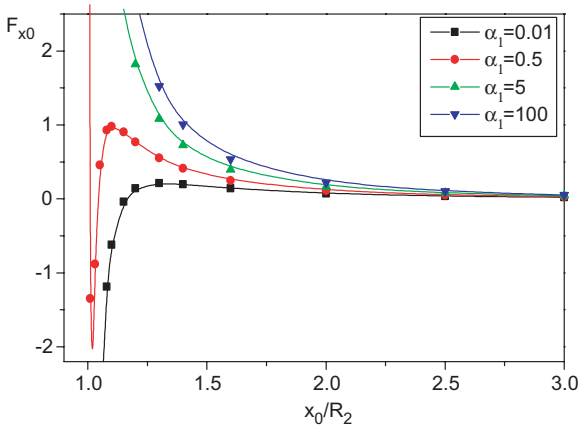

Fig. 3. Variation of the dislocation force in the matrix for various interphase layer elastic moduli. ($M_1 = 5M_3$, $e_{15}^{(2)} = e_{15}^{(3)}$, $R_1/R_2 = 0.9$, $F_{x0} = (2\pi R_2/C_{44}^{(3)}b_z^2)F_x$, $\alpha_1 = C_{44}^{(2)}/C_{44}^{(3)}$).

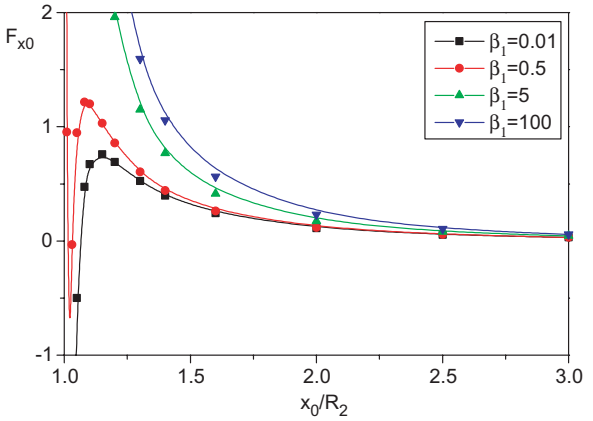

Fig. 4. Variation of the dislocation force in the matrix for various interphase layer piezoelectric moduli. ($M_1 = 5M_3$, $C_{44}^{(2)} = C_{44}^{(3)}$, $R_1/R_2 = 0.9$, $F_{x0} = (2\pi R_2/C_{44}^{(3)}b_z^2)F_x$, $\beta_1 = e_{15}^{(2)}/e_{15}^{(3)}$).

Now let us discuss the influence of the interphase layer parameters (electroelasticity modulus, thickness) on the image force. Here we take the piezoelectric screw dislocation vector $\mathbf{b} = \begin{Bmatrix} b_z \\ b_\varphi \end{Bmatrix} = \begin{Bmatrix} 1.0 \times 10^{-9}\ \text{m} \\ 1.0\ \text{V} \end{Bmatrix}$ (Lee et al., 2000). By means of Eqs. (82) and (84), the influence of the interphase layer parameters on the dislocation force are shown in Figs. 3–8.

Let us assume that matrix material is PZT-5H piezoelectric ceramics with the electroelastic properties:

$$M_3 = \begin{bmatrix} 3.53 \times 10^{10}\ \text{N/m}^2 & 17\ \text{C/m}^2 \\ 17\ \text{C/m}^2 & 1.51 \times 10^{-8}\ \text{C/Vm} \end{bmatrix}$$

and the dielectric modulus$d_{11}^{(1)} = d_{11}^{(2)}$. The variations of the dislocation force with respect to the location are depicted in Fig. 3 for various interphase layer elastic modulus and in Fig. 4 for various interphase layer piezoelectric modulus. It is seen that hard inclusion ($C_{44}^{(1)} > C_{44}^{(3)}$) and hard interphase layer ($C_{44}^{(2)} > C_{44}^{(3)}$)

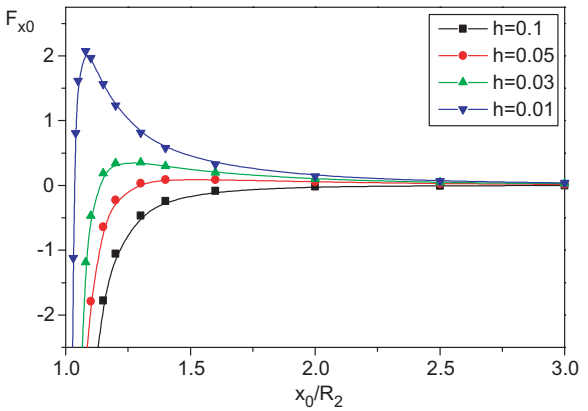

Fig. 5. Variation of the dislocation force in the matrix for various interphase layer thickness. ($M_1 = 5M_3$, $C_{44}^{(2)}/C_{44}^{(3)} = 0.2$, $e_{15}^{(2)}/e_{15}^{(3)} = 0.2$, $F_{x0} = (2\pi R_2/C_{44}^{(3)}b_z^2)F_x$, $h = (R_2 - R_1)/R_2$).

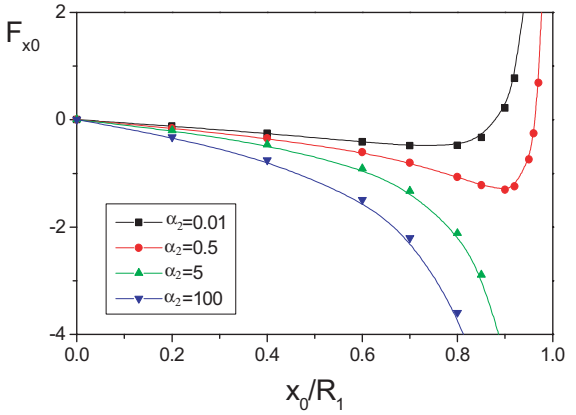

Fig. 6. Variation of the dislocation force in the inclusion for various interphase layer elastic moduli. ($M_3 = 5M_1$, $e_{15}^{(2)} = e_{15}^{(1)}$, $R_1/R_2 = 0.9$, $F_{x0} = (2\pi R_1/C_{44}^{(1)}b_z^2)F_x$, $\alpha_2 = C_{44}^{(2)}/C_{44}^{(1)}$).

repel the piezoelectric screw dislocation in the matrix. The hard inclusion ($C_{44}^{(1)} > C_{44}^{(3)}$) and the very soft interphase layer ($C_{44}^{(2)} \ll C_{44}^{(3)}$) may first attract the dislocation and then repel it with the increase of the distance between the dislocation and the interphase layer. An interesting result is that, for not very soft interphase, force on dislocation will be a large positive value when the dislocation approaches to the interphase layer from infinity along with the x-axis. For various piezoelectric moduli, Parallel results can be obtained in Figs. 4 and 5 illustrates the variation of the force on the dislocation located in the matrix with respect to the location for various interphase layer thickness. Noticeable, for the very thick interphase layer, the force on the dislocation is always negative (attract dislocation) as $C_{44}^{(2)} < C_{44}^{(3)}$ and $e_{15}^{(2)} < e_{15}^{(3)}$. The dislocation force is very large when the dislocation is closed to the mismatching interphase layer, whereas it has dropped down to very small when the distance between the dislocation and the interphase layer goes up to the double radius of the interphase layer.

Now let us assume that the inclusion material is PZT-5H piezoelectric ceramics with the electroelastic properties:

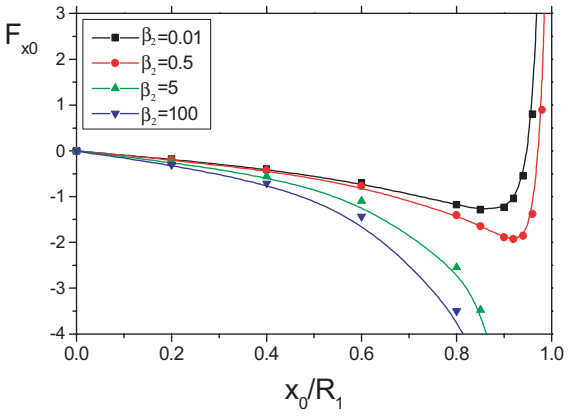

Fig. 7. Variation of the dislocation force in the inclusion for various interphase layer piezoelectric moduli. ($M_3 = 5M_1$, $C_{44}^{(2)} = C_{44}^{(1)}$, $R_1/R_2 = 0.9$, $F_{x0} = (2\pi R_1/C_{44}^{(1)}b_z^2)F_x$, $\beta_2 = e_{15}^{(2)}/e_{15}^{(1)}$).

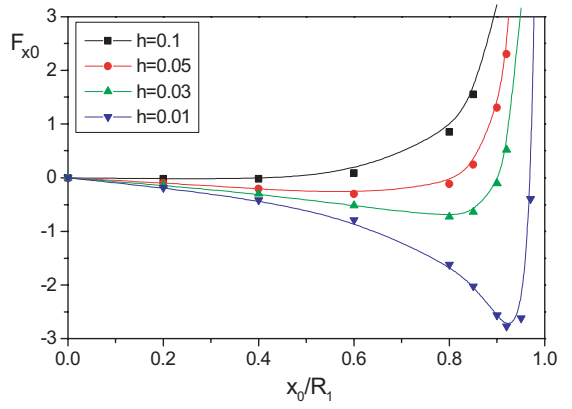

Fig. 8. Variation of the dislocation force in the inclusion for various interphase layer thickness. ($M_3 = 5M_1$, $C_{44}^{(2)}/C_{44}^{(1)} = 0.2$, $e_{15}^{(2)}/e_{15}^{(1)} = 0.2$, $F_{x0} = (2\pi R_1/C_{44}^{(1)}b_z^2)F_x$, $h = (R_2 - R_1)/R_1$).

$$M_1 = \begin{bmatrix} 3.53 \times 10^{10}\ \mathrm{N/m^2} & 17\ \mathrm{C/m^2} \\ 17\ \mathrm{C/m^2} & 1.51 \times 10^{-8}\ \mathrm{C/Vm} \end{bmatrix}$$

and the dielectric modulus $d_{11}^{(2)} = d_{11}^{(3)}$. The variations of the dislocation force in the inclusion with respect to the location are depicted in Fig. 6 for various interphase layer elastic modulus and in Fig. 7 for various interphase layer piezoelectric modulus. Similarly, it is seen that hard matrix ($C_{44}^{(3)} > C_{44}^{(1)}$) and hard interphase layer ($C_{44}^{(2)} > C_{44}^{(1)}$) repel the piezoelectric screw dislocation in the inclusion. The hard matrix ($C_{44}^{(3)} > C_{44}^{(1)}$) and the soft interphase layer ($C_{44}^{(2)} < C_{44}^{(1)}$) may first attract the dislocation and then repel it with the increase of the distance between the dislocation and the interphase layer. For various piezoelectric moduli, Parallel results can be obtained. Fig. 8 illustrates the variation of the force on the dislocation located in the inclusion with respect to the location for various interphase layer thickness. Similarly, for very thick interphase layer, the force on the dislocation is always positive (attract dislocation) as $C_{44}^{(2)} < C_{44}^{(1)}$ and $e_{15}^{(2)} < e_{15}^{(1)}$.The dislocation force is very large when the dislocation is closed to the mismatching interphase layer, whereas it vanishes in the center of the inclusion.

6.3. Interaction between a piezoelectric screw dislocation and a coated cylinder

A study on the interaction between a piezoelectric screw dislocation and a coated cylinder is useful in understanding the influence of a coating and a surface-bonded piezoelectric membrane on the dislocation force. In this case, let us assume piezoelectric, dielectric and elastic constants of the matrix are zero ($C_{44}^{(3)} = e_{15}^{(3)} = d_{11}^{(3)} = 0$). Then the image force can be obtained from Eq. (75) for the case of the piezoelectric screw dislocation located in the inclusion.

The variation of the image force in a coated cylinder with respect to the location are depicted in Fig. 9 for various interphase layer elastic modulus, in Fig. 10 for various interphase layer piezoelectric modulus and in Fig. 11 for various interphase layer thickness. The above figures and further analysis imply that the interphase electroelastic properties are the dominant factor of the image force on the dislocation for serious mismatching.

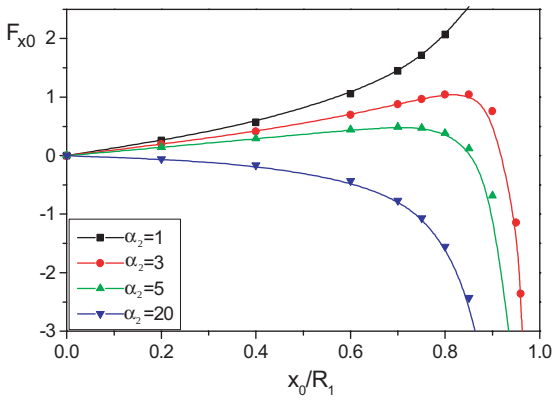

Fig. 9. Variation of the dislocation force in a coated cylinder for various coating elastic moduli. ($M_3 = 0$, $e_{15}^{(1)} = e_{15}^{(2)}$, $R_1/R_2 = 0.9$, $F_{x0} = (2\pi R_1/C_{44}^{(1)} b_z^2)F_x$, $\alpha_2 = C_{44}^{(2)}/C_{44}^{(1)}$).

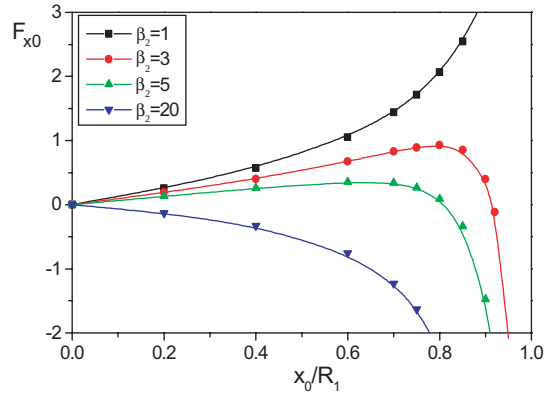

Fig. 10. Variation of the dislocation force in a coated cylinder for various coating piezoelectric moduli. ($M_3 = 0$, $C_{44}^{(2)} = C_{44}^{(1)}$, $R_1/R_2 = 0.9$, $F_{x0} = (2\pi R_1/C_{44}^{(1)} b_z^2)F_x$, $\beta_2 = e_{15}^{(2)}/e_{15}^{(1)}$).

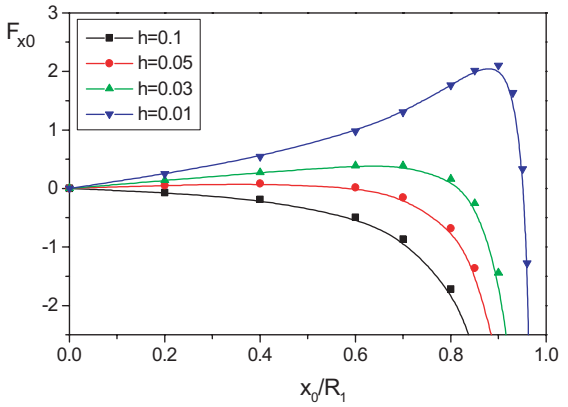

Fig. 11. Variation of the dislocation force in a coated cylinder for various coating thickness. ($M_3 = 0$, $C_{44}^{(2)}/C_{44}^{(1)} = 10$, $e_{15}^{(2)}/e_{15}^{(1)} = 10$, $F_{x0} = (2\pi R_1/C_{44}^{(1)}b_z^2)F_x$, $h = (R_2 - R_1)/R_1$).

7. Conclusions

An efficient method is developed for the BVP in multiplying connected regions, in terms of which the analytical solutions are obtained for a piezoelectric screw dislocation interacting with an interphase layer between the circular inclusion and the matrix. The results indicate that the interphase layer has significant effects on the Peach–Koehler dislocation force. The obtained explicit solutions can be used as Green's functions to solve the problem of electroelastic interaction between the coated inclusion and the arbitrary shape crack inside the matrix or inclusion under antiplane mechanical and inplane electric loadings at infinity. In addition, it can be used to study the crack growth in composites, as well as strengthening and hardening mechanisms in alloyed materials.

Acknowledgements

The authors would like to thank the support from the National Natural Science Foundation of China and the Natural Science Foundation of Hunan Province. In addition, the authors are grateful to the anonymous reviewers for their comments which have much improved this paper.

References

Barnett, D.M., Tetelman, A.S., 1966. The stress distribution produced by screw dislocation pile-ups at rigid circular cylindrical inclusions. Journal of Mechanics and Physics of Solids 14, 329–348.

Deng, W., Meguid, S.A., 1999. Analysis of a screw dislocation inside an elliptical inhomogeneity in piezoelectric solids. International Journal of Solids and Structures 36, 1449–1469.

Dundurs, J., Mura, T., 1964. Interaction between an edge dislocation and a circular inclusion. Journal of Mechanics and Physics of Solids 12, 177–189.

Dundurs, J., Sendeckyj, G.P., 1965. Edge dislocation inside a circular inclusion. Journal of Mechanics and Physics of Solids 13, 141–147.

Fang, Q.H., Liu, Y.W., Jiang, C.P., 2003. Edge dislocation interacting with an interfacial crack along a circular inhomogeneity. International Journal of Solids and Structures 40, 5781–5797.

Gong, S.X., Meguid, S.A., 1994. A screw dislocation interaction with an elastic elliptical inhomogeneity. International Journal of Engineering Science 32, 1221–1228.

Hirth, J.P., Lothe, J., 1982. Theory of dislocations, second ed. John-wiley, New York.
Huang, Z., Kuang, Z.B., 2001. Dislocation inside a piezoelectric media with an elliptical inhomogeneity. International Journal of Solids and Structures 38, 8459–8480.
Jiang, C.P., Tong, Z.H., Chueng, Y.K., 2001. A generalized self-consistent method for piezoelectric fiber reinforced composites under anti-plane shear. Mechanics of Materials 33, 295–308.
Jiang, C.P., Liu, Y.W., Xu, Y.L., 2003. Interaction of a screw dislocation in interphase layer with the inclusion and matrix. Applied Mathematics and Mechanics 22 (8), 979–988.
Kattis, M.A., Providas, E., Kalamkarov, A.L., 1998. Two-phone potentials in the analysis of smart composites having piezoelectric components. Composites Part B 29 (1), 9–14.
Lee, K.Y., Lee, W.G., Pak, Y.E., 2000. Interaction between a semi-infinite crack and a screw dislocation in a piezoelectric material. ASME Journal of Applied Mechanics 67, 165–170.
Liu, J.X., Jiang, Z.Q., Feng, W.J., 2000. On the electro–elastic interaction of piezoelectric screw dislocation with an elliptical inclusion in piezoelectric materials. Applied Mathematics and Mechanics 21, 1185–1190.
Liu, Y.W., Jiang, C.P., Cheung, Y.K., 2003. A screw dislocation interacting with an interphase layer between a circular inclusion and the matrix. International Journal of Engineering Science 41 (16), 1883–1898.
Liu, Y.W., Fang, Q.H., 2003. Electroelastic interaction between a piezoelectric screw dislocation and circular inhomogeneity interfacial rigid lines. International Journal of Solids and Structures 40, 5353–5370.
Luo, H.A., Chen, Y., 1991. An edge dislocation in a three-phase composites cylinder. ASME Journal of Applied Mechanics. 58, 75–86.
Muskhelishvili, N.L., 1975. Some Basic Problems of Mathematical Theory of Elasticity. Noordhoff, Leyden.
Meguid, S.A., Deng, W., 1998. Electro–elastic interaction between a screw dislocation and elliptical inhomogeneity in piezoelectric materials. International Journal of Solids and Structures 35, 1467–1482.
Pak, Y.E., 1990. Force on piezoelectric screw dislocation. ASME Journal of Applied Mechanics 57, 863–869.
Qaissaunee, M.T., Santare, M.H., 1995. Edge dislocation interaction with an elliptical inclusion surrounding by an interfacial zone. Quarter Journal Mechanics and Applied Mathematic 48, 465–482.
Smith, E., 1968. The interaction between dislocation and inhomogeneities-1. International Journal of Engineering Science 6, 129–143.
Sendeckj, G.P., 1970. Screw dislocation in inhomogeneity solids. In: Simmons, J.A.WitR.de, Bullough, R. (Eds.), Fundamental Aspects of Dislocation Theory. Nat. bur. stand., US.
Sudak, L.J., 2003a. On the interaction between a dislocation and a circular inhomogeneity with imperfect interface in antiplane shear. Mechanics Research Communications 30, 53–59.
Sudak, L.J., 2003b. Effect of an interphase layer on the electroelastic stresses within a three-phase elliptic inclusion. International Journal of Engineering Science 41, 1019–1039.
Tiersten, H.F., 1969. Linear Piezoelectric Plate Vibrations. Plenum Press, New York.
Xiao, Z.M., Chen, B.J., 2000. A screw dislocation interacting with a coated fiber. Mechanics of Materials 37, 485–494.
Xiao, Z.M., Chen, B.J., 2001. On interaction between an edge dislocation and a coated inclusion. International Journal of Solids and Structures 38, 2533–2548.
Xiao, Z.M., Chen, B.J., 2002. A screw dislocation interacting with inclusions in fiber–reinforced composites. Acta Mechanica 155, 203–214.
Wang, X., Shen, Y.P., 2001. Arc interface crack in a three-phase piezoelectric composites constitutive model. Acta Mechanica Solids Sinica 22, 329–342.
Wang, X., Shen, Y.P., 2002. An edge dislocation in a three-phase composite cylinder model with a sliding interface. ASME Journal of Applied Mechanics 69, 527–538.
Zhang, T.Y., Qian, C.F., 1996. Interaction of a screw dislocation with a thin-film covered mode III crack. Acta Metallurgica Materiala 39, 2739–2744.